

# Waveguide Leaky-Wave Antennas: Modal Configuration and Dispersion Properties

*Filippo Costa and Giuliano Manara*

*Abstract* – Radiating modes supported by waveguide-based leaky-wave antennas are analyzed in terms of field distribution and a propagation constant. An analytic approach for computing the propagation constant of transverse electric modes in the partially open waveguide and on the basis of the transverse resonance method is presented, making use of a dielectric cover and a partially reflective surface cover.

## 1. Introduction

Leaky-wave antennas (LWA) are designed by suitably controlling the leakage rate of a guiding structure [1]. A simple structure that is typically used to synthesize leaky antennas consists of a Fabry–Perot (FP) cavity. The FP cavity typically consists of two partially reflective surfaces (PRSs) that can create constructive interferences at the resonance frequencies of the cavity [2]. By using the image theorem, the same effects can be obtained with a single PRS located above a perfectly conducting ground plane. The working frequency of the leaky antenna corresponds roughly to the first resonance point of the cavity that can be computed with a simple ray optic approach. However, to gain a deeper understanding of the antenna radiation mechanism, the behavior of the modal propagation constant has to be determined. The propagation constant of each mode inside the FP cavity is a complex quantity: the real part represents the phase constant of the traveling wave and the imaginary part is related to the leakage rate of the wave power, which is gradually lost by the cavity when radiated in free space. Depending on the specific configuration of the cavity, different modes are supported, and typically, one of them is used to synthesize the leaky antenna. The FP cavity can be synthesized both in a bidimensional and unidimensional fashion [3]. In the former case, a source is placed in the center of the cavity, and a directive pattern is achieved on both planes. In the latter case, the source is placed in the center of a shielded cavity, obtaining a fan beam with a high directivity along one direction. In both cases, multiple sources [3–6] can be used to better illuminate the cavity or to obtain array thinning.

## 2. Radiation Mechanism

The LWA is a traveling wave antenna characterized by a wave guided through an electromagnetic (EM)

structure that releases energy gradually into the surrounding space. The energy release is obtained by replacing a part of the guiding structure with a surface that is partially reflecting and partially transmitting. The PRS can be synthesized either with a uniform dielectric [1], with a relatively high permittivity, or, for instance, with a metasurface. When the guiding structure is partially opened, the propagation constant inside the structure becomes complex because both delay and leakage are experienced by the traveling wave. The complex propagation constant is characterized by a real part  $\beta_z$ , which accounts for the phase delay of the wave, and an imaginary part  $\alpha_z$ , which is related to the energy leakage:

$$k_z = \beta_z - j\alpha_z \quad (1)$$

A bidimensional sketch of the traveling wave radiation and the radiation direction is shown in Figure 1. If  $\alpha$  is small compared with  $\beta$ , the radiation direction  $\theta$  can be computed as

$$\theta = \cos^{-1}\left(\frac{\beta_z}{k_0}\right) \quad (2)$$

where  $k_0$  is the free-space propagation constant.

The antenna can be interpreted also as the FP cavity by using ray optics [2, 7, 8]: in this case, the leaky waves are represented by the rays bouncing from the top to the bottom of the cavity and vice versa, gradually releasing in-phase electric fields. The cavity can be excited by a small nondirective antenna, which can be a dipole, a patch antenna, a waveguide, or another type of source. Each type of source is characterized by a specific configuration of the EM fields and thus will excite a particular modal configuration inside the FP cavity. Modal configurations for a shielded waveguide FP cavity are analyzed in Section 4.

## 4. Radiating Modes

In the configuration shown in Figure 2, the top wall of the waveguide is replaced by a PRS; thus, the cavity is allowed to radiate toward the  $y$  direction. According to Figure 2, the height of the waveguiding structure is named  $b$ , and the width is named  $a$ . Once fixed, the height  $b$ , for instance, to 15 mm, the number of propagating modes is determined by the width  $a$ . The propagating modes for two waveguide configurations with  $a$  equal to 21 mm (WG1) or 10 mm (WG2) are summarized in Table 1. In WG1, the first propagating mode is the transverse electric ( $TE_{10}$ ), and the second mode is  $TE_{01}$ . The former mode is radiating if the top of the waveguide is perforated with an array of slots

Manuscript received 30 June 2020.

Filippo Costa and Giuliano Manara are with the Microwave and Radiation Laboratory, University of Pisa, Via Caruso 16, 56122 Pisa, Italy; e-mail giuliano.manara@unipi.it.

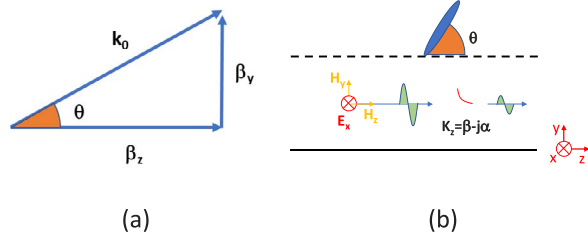


Figure 1. (a) Propagation constant and radiation angle of the leaky wave and (b) bidimensional sketch of the TE mode propagation inside the FP cavity and radiation pattern.

because the current flowing of the waveguide is interrupted [9]. However, using this mode configuration does not allow us to synthesize a broadside antenna, even with a central feed. The second mode  $TE_{01}$  is, instead, useful for radiation because the propagation constant has a nonzero component along the  $y$  direction. Therefore, the cavity width can be reduced to  $a = 10$  mm (WG2) so that the first mode cut-off frequency can be moved above that of the radiating mode, thus avoiding that part of the energy is coupled with the  $TE_{10}$  mode.

In this case, the  $TE_{01}$  mode becomes the fundamental mode supported by the waveguide WG2. Note that the  $TE_{01}$  mode of WG2 can be seen as the fundamental mode ( $TE_{10}$ ) of a conventional rectangular waveguide, rotated by  $90^\circ$  with respect to WG1, so its larger side becomes parallel to the  $y$ -axis. This ensures the energy to be radiated from the top side of the cavity once the metallic wall is replaced by the PRS. This antenna configuration allows us to radiate the broadside by using a waveguide feed from the bottom side with the electric field oriented along the  $x$  direction. Indeed, radiation occurs through the smaller side of the standard rectangular waveguide rotated  $90^\circ$ .

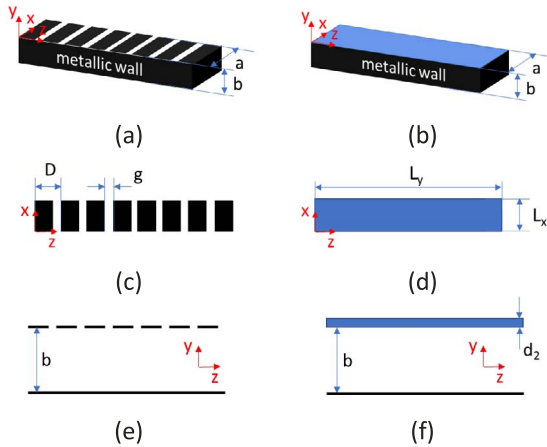


Figure 2. (a) Perspective view, (c) top view, and (e) side view of the unidimensional shielded cavity closed with a PRS. (b) Perspective view, (d) top view, and (f) side view of the unidimensional shielded cavity closed with a dielectric.

Table 1. Cut-off frequencies of the first three modes in WG1 and WG2 configurations

	$a$ (mm)	$b$ (mm)	Mode	$TE_{10}$	$TE_{01}$	$TE_{11}$
WG1	21	15	$f_c$	7.14	10	12.8
WG2	10	15	$f_c$	15	10	18

## 5. Propagation Constant Calculation

The frequency behavior of both the real part and the imaginary part of the propagation constant of the guided leaky waves can be computed by solving the dispersion equation obtained with the transverse resonance method [10]:

$$Z_{\text{down}} + Z_{\text{up}} = 0 \quad (3)$$

The transverse transmission line models (along the  $y$  direction) of the FP cavity, both for the dielectric cover and the FSS cover, are shown in Figures 3a and 3b, respectively. The transcendental function in (3) can be solved both for the TE and Transverse Magnetic (TM) modes. The derived propagation constant is a good approximation of the real structures reported in Figure 2 (assuming that the metallic side walls extend to infinity in the  $y$  direction). We derive the solution of the equation for TE-polarized modes because they are used to synthesize the leaky antenna. The impedance  $Z_{\text{down}}$  is defined as

$$Z_{\text{down}}^{\text{TE}} = jZ_0^{\text{TE}} \tan(k_{y1}b) \quad (4)$$

The impedance  $Z_{\text{up}}$  in case of the dielectric cover is

$$Z_{\text{up}}^{\text{TE}} = Z_2^{\text{TE}} \frac{Z_0^{\text{TE}} + jZ_2^{\text{TE}} \tan(k_{y2}d_2)}{Z_2^{\text{TE}} + jZ_0^{\text{TE}} \tan(k_{y2}d_2)} \quad (5)$$

where  $Z_2^{\text{TE}} = (\omega\mu_0)/k_{y2}$  is the characteristic impedance of the superstrate along the  $y$  direction, with  $k_{y2} = \sqrt{k_0^2 \epsilon_{r2} - k_z^2}$ ,  $Z_0^{\text{TE}} = (\omega\mu_0)/k_{y0}$ , and  $k_{y0} = \sqrt{k_0^2 - k_z^2}$ . Also,  $d_2$  and  $\epsilon_{r2}$  are the thickness and the relative dielectric permittivity of the superstrate,  $\omega$  is the angular frequency, and  $\epsilon_0$  and  $\mu_0$  are the dielectric permittivity and magnetic permeability of free space, respectively. The impedance  $Z_{\text{up}}$  for the FSS case is

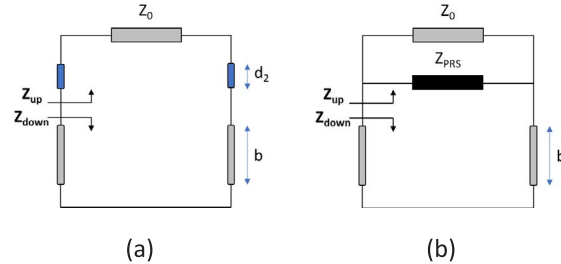


Figure 3. Transmission line models (along the  $y$  direction) of the cavity with (a) the dielectric cover and with (b) the PRS cover.

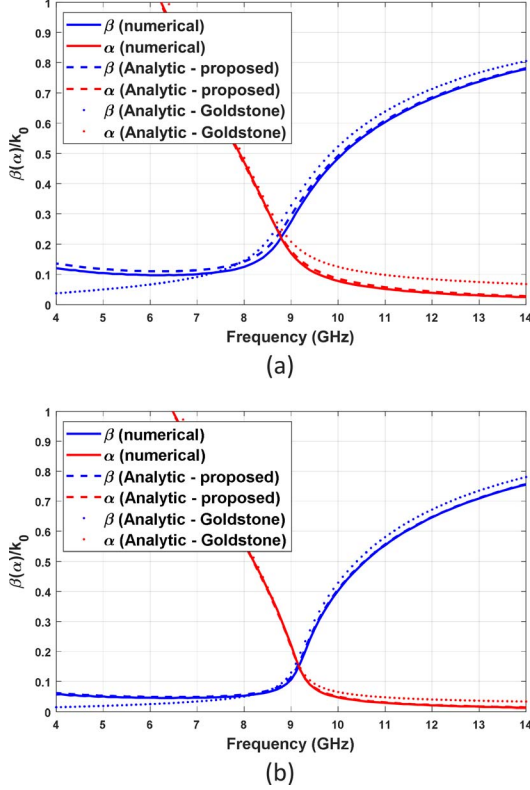


Figure 4. Normalized leaky-wave phase ( $\beta_z/k_0$ ) and attenuation ( $\alpha_z/k_0$ ) constants as a function of frequency for the relevant TE leaky mode of the LWA. Inductive grid PRS superstrate: (a)  $D = 5$  mm and  $g = 0.15$  mm and (b)  $D = 5$  mm,  $g = 0.5$  mm.

$$Z_{\text{up}}^{\text{TE}} = Z_{\text{PRS}}^{\text{TE}} // Z_0^{\text{TE}} \quad (6)$$

Thus, (3) can be solved numerically by searching the zeros of the dispersion equation in the complex plane. One approach consists of searching the solutions for high-frequency points, located close to the real axis, by perturbing the closed waveguide solution. The remaining lower frequency points can be derived iteratively [3]. Approximate analytical expressions of the leaky-wave complex propagation constant can also be derived by using different strategies. The approach proposed in [11] was based on a perturbation expansion of the closed ideal waveguide propagation constant, when one of the faces was substituted by a PRS. An alternative expression can be derived by assuming that the cavity height is approximately  $h_1 \approx n\lambda/2$ , where  $n$  is an integer number [12].

By using this hypothesis,  $Z_{\text{down}}$  in (4) can be approximated as

$$Z_{\text{down}}^{\text{TE}} \simeq jZ_0^{\text{TE}}(k_{y1}b + n\pi) \quad (7)$$

where  $b$  is the cavity height. An approximation for the upper impedance  $Z_{\text{up}}$  for the dielectric cover can be obtained by using the approximation of a quarter wavelength impedance transformer [12] ( $Z_{\text{up}}^{\text{TE/TM}} = Z_0^{\text{TE/TM}}/\varepsilon_{r2}$ ). By using the aforementioned

simplifications, an analytical expression of the TE propagation constant in the  $y$  direction can be derived [12]:

$$k_y^{\text{TE}} = \frac{\pi\lambda_0}{2h_1^2} \left( 2\frac{h_1}{\lambda_0} + j\frac{\pi}{\varepsilon_{r2}} \right) \quad (8)$$

For the PRS superstrate, the upper impedance  $Z_{\text{up}}$  is computed as the parallel connection of the PRS impedance and the free-space impedance. If the angular variation of the free-space impedance is retained, an accurate expression of the normal component of the propagation constant is derived [3]

$$k_y^{\text{TE}} = \frac{1}{2bZ_{\text{PRS}}^{\text{TE}}} \left[ - (b\mu_0\omega - Z_{\text{PRS}}^{\text{TE}}(\pi + j)) + \sqrt{(b\mu_0\omega - Z_{\text{PRS}}^{\text{TE}}(\pi + j))^2 + 4\pi(bZ_{\text{PRS}}^{\text{TE}})\mu_0\omega} \right] \quad (9)$$

where  $Z_{\text{PRS}}^{\text{TE}}$  represents the PRS impedance at normal incidence. Note that the dependence of the PRS impedance on the angle is not considered in this expression, because for the inductive grid superstrate, the impedance is independent of the incidence angle for TE polarization [13]. For the dielectric-filled cavity, an analytic expression can be derived by neglecting the dependence of the free-space impedance on the surface wave propagation constant  $k_z$ . In this case, the normal propagation constant is

$$k_y^{\text{TE}} = j \frac{(Z_{\text{PRS}}^{\text{TE}} + \zeta_0)\omega\mu_0\pi}{\zeta_0 Z_{\text{PRS}}^{\text{TE}} + j\omega\mu_0 b(Z_{\text{PRS}}^{\text{TE}} + \zeta_0)} \quad (10)$$

Once the propagation constant is computed along the normal direction, the leaky-wave propagation constant is obtained as  $k_z^{\text{TE}} = \beta_z - j\alpha_z = \sqrt{\varepsilon_{r1}k_0^2 - (k_y^{\text{TE}})^2}$ . The accuracy of the analytical expressions is checked in Figure 4 for two different grids parameters. The curves obtained through analytic expressions are compared with the curves derived by numerically solving the transcendental equation in (3). As the reflectivity of the grid decreases (more leakage), the accuracy of the perturbation approach proposed in [11] deteriorates more rapidly than the analytic expression proposed in (9). For sake of comparison, in both cases, we used the same expressions for the grid impedance [13]. The dielectric-filled cavity case is reported in Figure 5. The case of the air-filled cavity with dielectric cover is reported in Figure 6, where the numerical solution is compared with the propagation constant derived through relation (8).

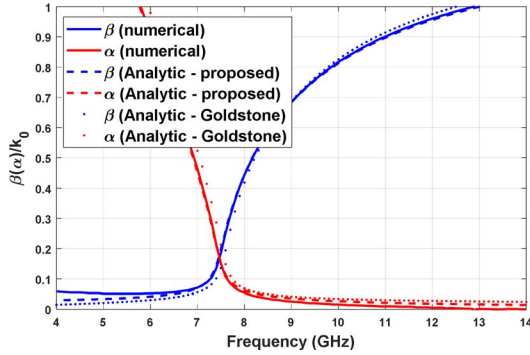


Figure 5. Normalized leaky-wave phase ( $\beta_z/k_0$ ) and attenuation ( $\alpha_z/k_0$ ) constants as a function of frequency for the relevant TE leaky mode of the LWA. Inductive grid superstrate:  $D = 5$  mm and  $g = 0.5$  mm. The cavity is filled with the dielectric ( $\epsilon_r = 1.5$ ).

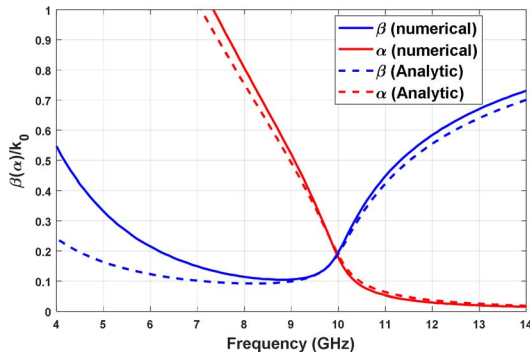


Figure 6. Normalized leaky-wave phase ( $\beta_z/k_0$ ) and attenuation ( $\alpha_z/k_0$ ) constants as a function of frequency for the relevant TE leaky mode of the LWA. Dielectric superstrate:  $\epsilon_r = 9$  and  $d_2 = 2.5$  mm.

## 6. Conclusion

Some analytical expressions for computing the propagation constants of waveguide-based LWA have been presented. Both cases of dielectric and PRS covers have been considered.

## 7. References

1. D. R. Jackson, C. Caloz, and T. Itoh, "Leaky-Wave Antennas," *Proceedings of the IEEE*, **100**, 7, July 2012, pp. 2194-2206.

2. A. P. Feresidis, G. Goussetis, S. Wang, and J. C. Vardaxoglou, "Artificial Magnetic Conductor Surfaces and Their Application to Low-Profile High-Gain Planar Antennas," *IEEE Transactions on Antennas and Propagation*, **53**, 1, January 2005, pp. 209-215.
3. F. Costa, D. Bianchi, A. Monorchio, and G. Manara, "Linear Fabry-Perot/Leaky-Wave Antennas Excited by Multiple Sources," *IEEE Transactions on Antennas and Propagation*, **66**, 10, October 2018, pp. 5150-5159.
4. R. Gardelli, M. Albani, and F. Capolino, "Array Thinning by Using Antennas in a Fabry-Perot Cavity for Gain Enhancement," *IEEE Transactions on Antennas and Propagation*, **54**, 7, July 2006, pp. 1979-1990.
5. D. Blanco, E. Rajo-Iglesias, S. Maci, and N. Llombart, "Directivity Enhancement and Spurious Radiation Suppression in Leaky-Wave Antennas Using Inductive Grid Metasurfaces," *IEEE Transactions on Antennas and Propagation*, **63**, 3, March 2015, pp. 891-900.
6. D. Comite, S. K. Podilchak, M. Kuznetsov, V. G. Buendía, P. Burghignoli, et al., "Wideband Array-Fed Fabry-Perot Cavity Antenna for 2-D Beam Steering," *IEEE Transactions on Antennas and Propagation*, July 2020, doi: 10.1109/TAP.2020.3008764.
7. G. V. Trentini, "Partially Reflecting Sheet Arrays," *IRE Transactions on Antennas and Propagation*, **4**, 4, October 1956, pp. 666-671.
8. F. Costa and A. Monorchio, "Design of Subwavelength Tunable and Steerable Fabry-Perot/Leaky Wave Antennas," *Progress in Electromagnetics Research*, **111**, Xxx 2011, pp. 467-481, doi: 10.2528/PIER10111702.
9. J. Liu, D. R. Jackson, and Y. Long, "Modal Analysis of Dielectric-Filled Rectangular Waveguide With Transverse Slots," *IEEE Transactions on Antennas and Propagation*, **59**, 9, September 2011, pp. 3194-3203.
10. G. Lovat, P. Burghignoli, and D. R. Jackson, "Fundamental Properties and Optimization of Broadside Radiation From Uniform Leaky-Wave Antennas," *IEEE Transactions on Antennas and Propagation*, **54**, 5, May 2006, pp. 1442-1452.
11. L. Goldstone and A. Oliner, "Leaky-Wave Antennas I: Rectangular Waveguides," *IRE Transactions on Antennas and Propagation*, **7**, 4, October 1959, pp. 307-319.
12. A. Neto and N. Llombart, "Wideband Localization of the Dominant Leaky Wave Poles in Dielectric Covered Antennas," *IEEE Antennas and Wireless Propagation Letters*, **5**, 1, December 2006, pp. 549-551.
13. O. Luukkonen, C. Simovski, G. Granet, G. Goussetis, D. Lioubtchenko, et al., "Simple and Accurate Analytical Model of Planar Grids and High-Impedance Surfaces Comprising Metal Strips or Patches," *IEEE Transactions on Antennas and Propagation*, **56**, 6, June 2008, pp. 1624-1632.